ELSEVIER

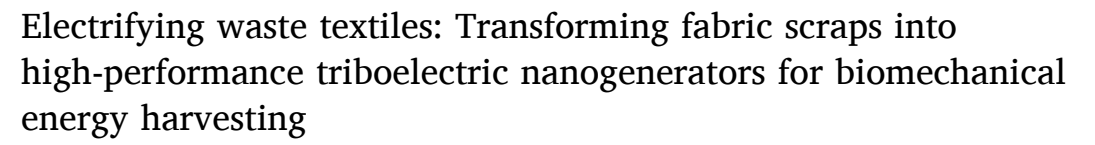
Contents lists available at ScienceDirect

Waste Management

journal homepage: www.elsevier.com/locate/wasman



Research Paper



Sebghatullah Amini ^a, Rumana Farheen Sagade Muktar Ahmed ^a, Santosh Kumar ^b, Sangamesha Madanahalli Ankanathappa ^c, Krishnaveni Sannathammegowda ^{a,*}

- ^a Department of Studies in Physics, University of Mysore, Mysuru 570006, Karnataka, India
- ^b Department of Education in Science and Mathematics, Regional Institute of Education Bhopal, Madhya Pradesh, India
- ^c Department of Chemistry, The National Institute of Engineering, Mysuru 570008, Karnataka, India

ARTICLE INFO

Keywords: Triboelectric nanogenerators Textile fabrics Energy harvesting Self-powered devices Wearable technology Waste management

ABSTRACT

Textiles are an integral part of daily life globally, but their widespread use leads to significant waste generation. Repurposing these discarded fabrics for energy harvesting offers a sustainable solution to both energy demand and textile waste management. In this study, Textile-based Triboelectric Nanogenerators (T-TENGs) were developed using recycled cloth as tribopositive layers and polyvinyl chloride (PVC) film as the tribonegative layer, with aluminum foil tape serving as electrodes. Five different recycled textiles were evaluated, and Scanning Electron Microscopy (SEM) and Energy-Dispersive X-ray Spectroscopy (EDS) analysis revealed a correlation between yarn structure and carbon content, leading to enhanced triboelectric performance. Silk-based TENG (S-TENG) demonstrated the highest output, with 320.76 V and 8.73 µA, while exhibiting stable performance over 10,000 cycles. Practical applications were explored by integrating T-TENGs into shoe insoles for energy harvesting during walking and jumping, with rayon-based TENG generating up to 208.52 V on a PVC coil mat. This work highlights the dual benefits of waste reduction and sustainable energy applications, making a compelling case for advanced technologies where recycled textiles function as frictional materials to harvest mechanical energy from human motion and convert it into electrical energy for use in flexible sensors and wearable devices.

1. Introduction

The textile industry, a significant component of the global manufacturing sector, plays a crucial role in the economy and social well-being of today's world (Jiang et al., 2023; Köksal et al., 2017). However, due to its diverse and heterogeneous nature, which spans from fiber transformation into yarns and fabrics to the production of various products such as synthetic yarns, wool, linen, geo-textiles, and clothing, it generates substantial negative environmental and social impacts (Huygens et al., 2023; Senthil Kumar and Suganya, 2017). Compared to most other industries, the global warming potential of textile production is notably higher, as vast quantities of landfilled textiles decompose into greenhouse gasses and contaminate groundwater (Dickson et al., 2014; Niinimäki et al., 2020). Also, biodegradable textile waste yields methane, a potent greenhouse gas that exacerbates global warming, while non-biodegradable and toxic synthetic materials pose

immeasurable environmental hazards (Alves et al., 2024; Roy Choudhury, 2013; Ye et al., 2023). Global textile consumption is projected to increase from 62 million tons to 102 million tons by 2030, leading to a corresponding rise in textile waste (Wagaw and Babu, 2023). The United States produces 16.2 million tons of textile waste annually, in which 15 % is recycled (Candido, 2021). In China, only 3.5 million tons of textile waste are recycled, despite 45 % of the total textile waste being discarded (Li et al., 2021). The European Union generates 16 million tons of textile waste, and recycling is only 26 % (Stanescu, 2021). Canada disposes 0.5 million tons of apparel waste (Juanga-Labayen et al., 2022), whereas India produces about 6.23 million tons of textile waste annually (Agrawal and Sharan, 2015). This escalating textile waste highlights the urgent need for more efficient recycling procedures, which are not only environmentally important but also economically necessary.

Extracting energy from recycled textile materials is a sustainable and smart approach to address energy needs and waste management.

E-mail address: sk@physics.uni-mysore.ac.in (K. Sannathammegowda).

^{*} Corresponding author.

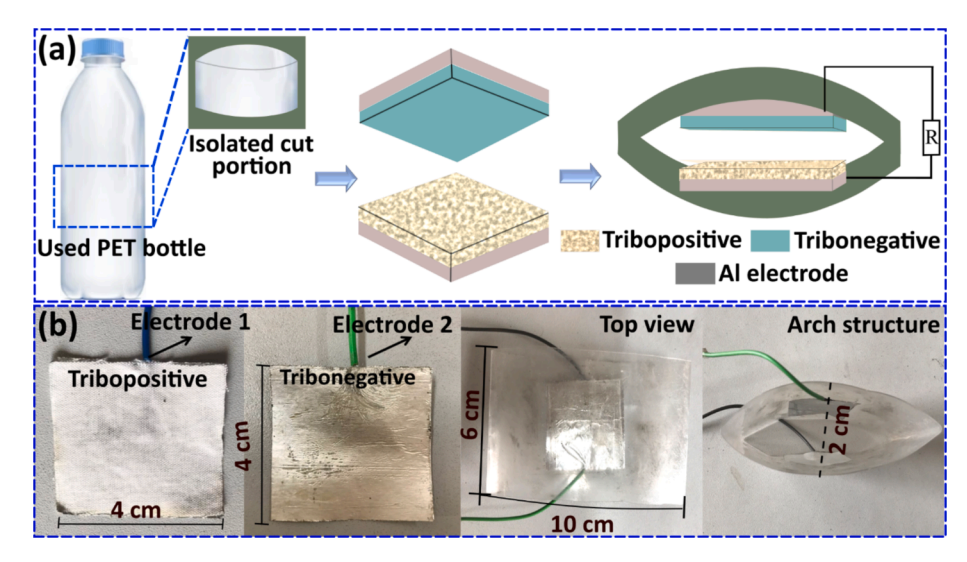


Fig. 1. (a) The schematic illustration of T-TENG fabrication. (b) The real images of the device.

Various technologies and methods have been applied to harness energy from recycled textiles, including incineration (Nunes et al., 2018), anaerobic digestion (Kumar et al., 2020), gasification (Arafat and Jijakli, 2013), landfill gas recovery (Wang, 2010), pyrolysis (Yousef et al., 2019), and many more. Even though these technologies offer potential benefits, they also present challenges including technological complexity, cost implications, and environmental concerns (Athanasopoulos and Zabaniotou, 2022; Khandaker et al., 2022). Moreover, not all types of waste materials are compatible with every recycling or disposal method; therefore, technology selection depends on the specific type of waste and the desired energy outcomes (Ahmed et al., 2024).

A promising solution to these challenges is the use of triboelectric nanogenerators (TENGs). TENGs can convert mechanical energy from scrap textiles into electrical energy through contact electrification and electrostatic induction (Amini et al., 2024; Dong et al., 2022b). This innovative technology is relatively low-cost, environmentally friendly (Amini et al., 2023), and can be integrated into various textile products, making it a versatile option for energy generation from waste textiles. Previous research focused on embedding TENGs into traditional textile frameworks using materials like conductive yarns (Wang et al., 2021), elastomers (Chen et al., 2016), and piezoelectric yarns (Dong et al., 2018), laying the groundwork for subsequent breakthroughs. Additionally, engineered textile architectures have been explored to integrate textile-based TENGs with enhanced mechanical robustness, washability, and comfort, making them suitable for practical applications ranging from self-powered wearables to healthcare monitoring systems (Dong et al., 2022a; Paosangthong et al., 2019). Despite significant progress, challenges remain, including the development of scalable manufacturing techniques, exploration of novel textile architectures and integration strategies along with waste management. Also, characterizing and modeling the mechanical and electrical behavior of textile-based TENGs under real-world conditions is crucial.

Here, in the present study, A range of recycled cloth samples have been employed, including linen (L), cotton (C), rayon (R), polyester (P), and silk (S), all sourced from local tailor shops. This variety not only demonstrates the applicability of different types of waste textiles but also highlights their distinct contributions from material optimization to TENG performance. Engineered T-TENGs with PVC film and aluminum (Al) foil tape demonstrates how waste materials can be effectively integrated into various TENG architectures such as vertical contact-separation and single-electrode modes. Notably, the silk-based TENG (S-TENG) generated a peak-to-peak output voltage of 320.76 V and a current of 8.73 μ A, which was used to charge electrolytic capacitors and

power a series of green light emitting diodes (LEDs). Practical applications are showcased by the integration of single electrode mode T-TENGs into everyday items such as shoe insoles, illustrating their potential to harness biomechanical energy from activities like walking and jumping on various surfaces, where rayon-based TENG generates up to 208.52 V on PVC coil mat. Thus, the current approach addresses the dual problem of the environmental challenge of textile waste and leverages the inherent characteristics of different fabrics to enhance TENG performance to both ecological and technological advancements.

2. Experimental Section

2.1. Materials

PVC powder, and tetrahydrofuran (THF) solvent were purchased from Central Drug House (P) Ltd, New Delhi, India. The waste cloth samples are collected from tailor shops in Mysore, Karnataka, India. Al foil tape was purchased commercially.

2.2. T-TENG fabrication

The schematic illustration of the T-TENG device fabrication is provided in Fig. 1a. To fabricate the device, a portion of a used Polyethylene terephthalate (PET) water bottle was cut vertically into dimensions of 6 cm \times 10 cm and used to house the triboelectric layers. The PET water bottle serves as a substrate, enhancing the mechanical durability of the device, while its insulating properties prevent charge leakage. The PVC film was achieved as reported in our previous study (Ahmed et al., 2023).

The PVC film was cut to dimensions of 4 cm \times 4 cm, and pasted onto the surface of Al foil tape and used as the top tribonegative layer. Waste cloth samples were washed two times with deionized water and dried at room temperature for 24 h. The samples were cut to the same dimensions and pasted onto the surface of Al foil tape without further physical or chemical modification and served as the bottom tribopositive layer of the T-TENGs. While Al foil tape serves as both the top and bottom electrodes of the devices. Real photographic images of the device are shown in Fig. 1b, showcasing the bottom tribopositive and top tribonegative layers, along with top and arch views of the device structure, offering a comprehensive visual representation of the T-TENG's design.

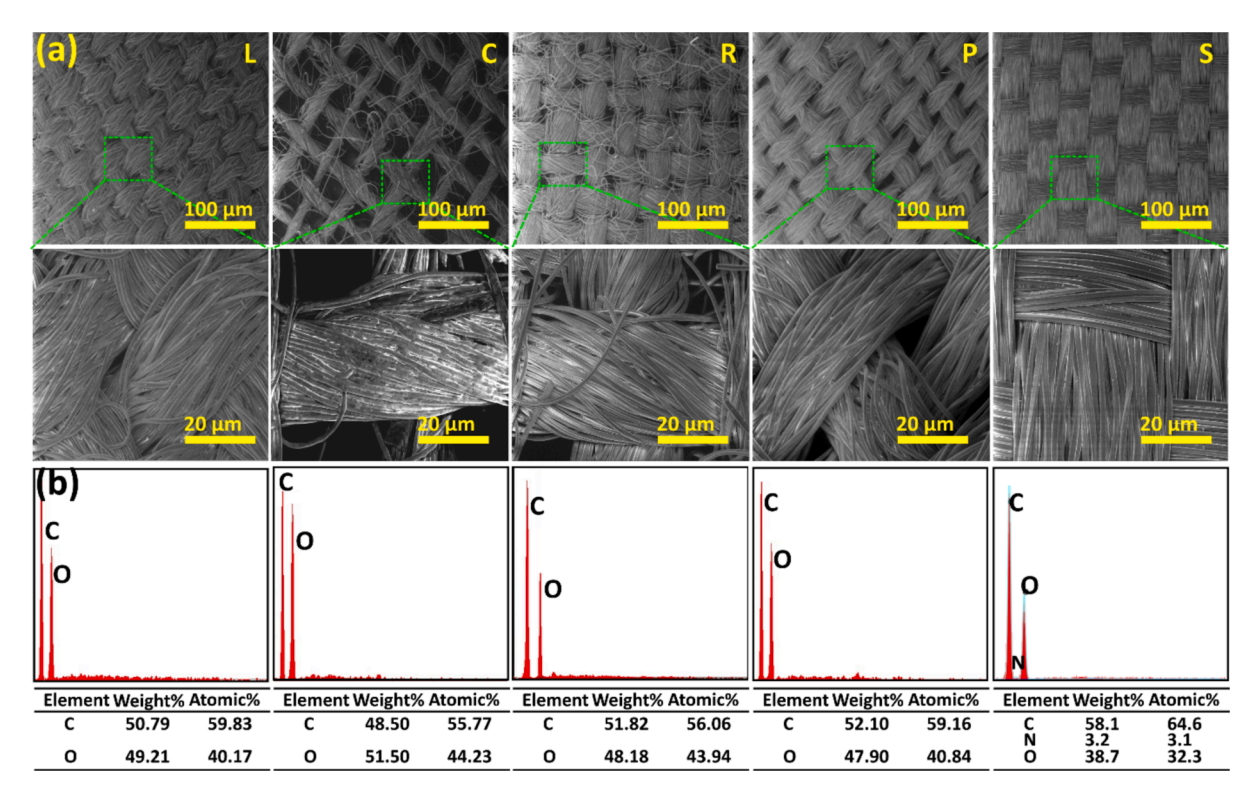


Fig. 2. (a) The SEM images and (b) the EDS spectrum of different textile fabric samples.

2.3. Characterization and electrical measurements

The investigation into the surface morphologies and elemental compositions of the textile samples was conducted utilizing Scanning Electron Microscopy coupled with Energy-Dispersive X-ray Spectroscopy (SEM-EDS, Zeiss, EVOLS15, Germany). This methodical approach allowed for the detailed observation and analysis of the surface structures and chemical constituents of the samples. Further, the electrical characteristics of the T-TENG devices were quantitatively assessed using a Source Measure Unit (SMU, Keithley, model 2460, USA). To evaluate

the long-term operational stability of the devices, a custom-engineered linear motor was employed. During these stability assessments, the maximum separation distance between the two triboelectric layers was maintained at 2 cm with the frequency of the contact-separation cycle set at 7 Hz. This comprehensive evaluation encompasses structural, compositional and functional assessments of the T-TENG devices, providing a robust framework for understanding their performance characteristics and operational durability.

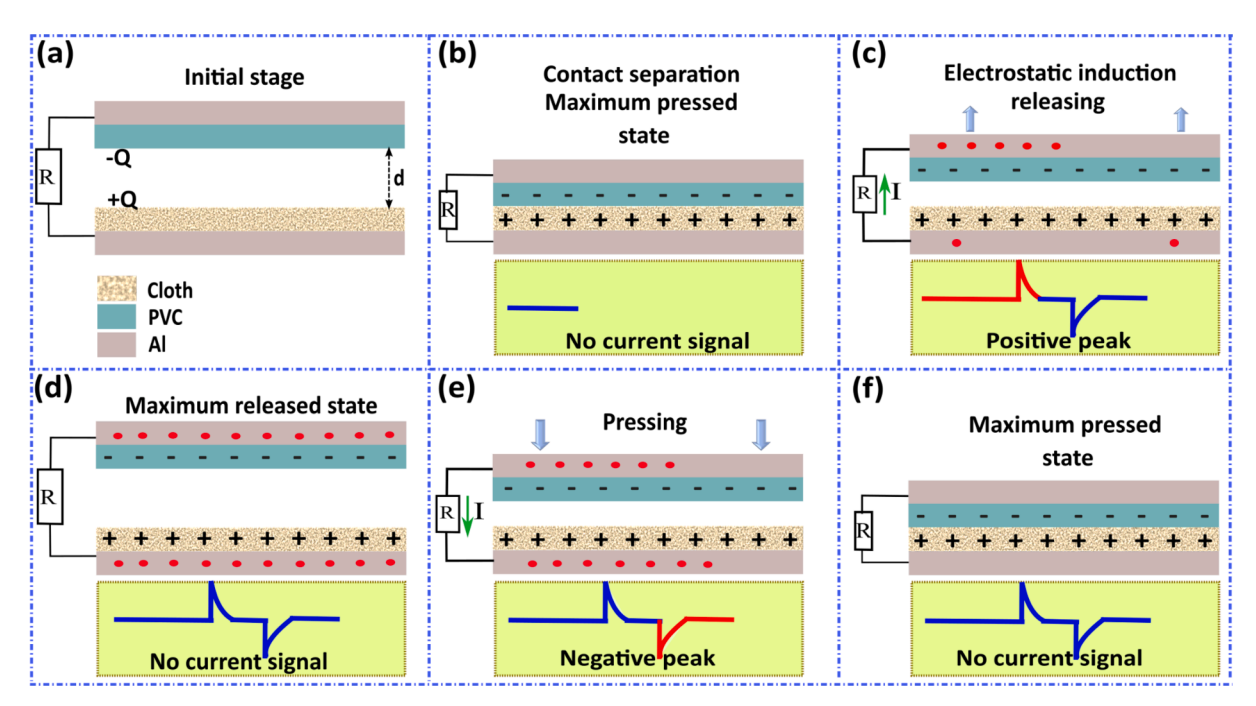


Fig. 3. (a) The schematic representation of T-TENG. (b-f) Working mechanism of the device.

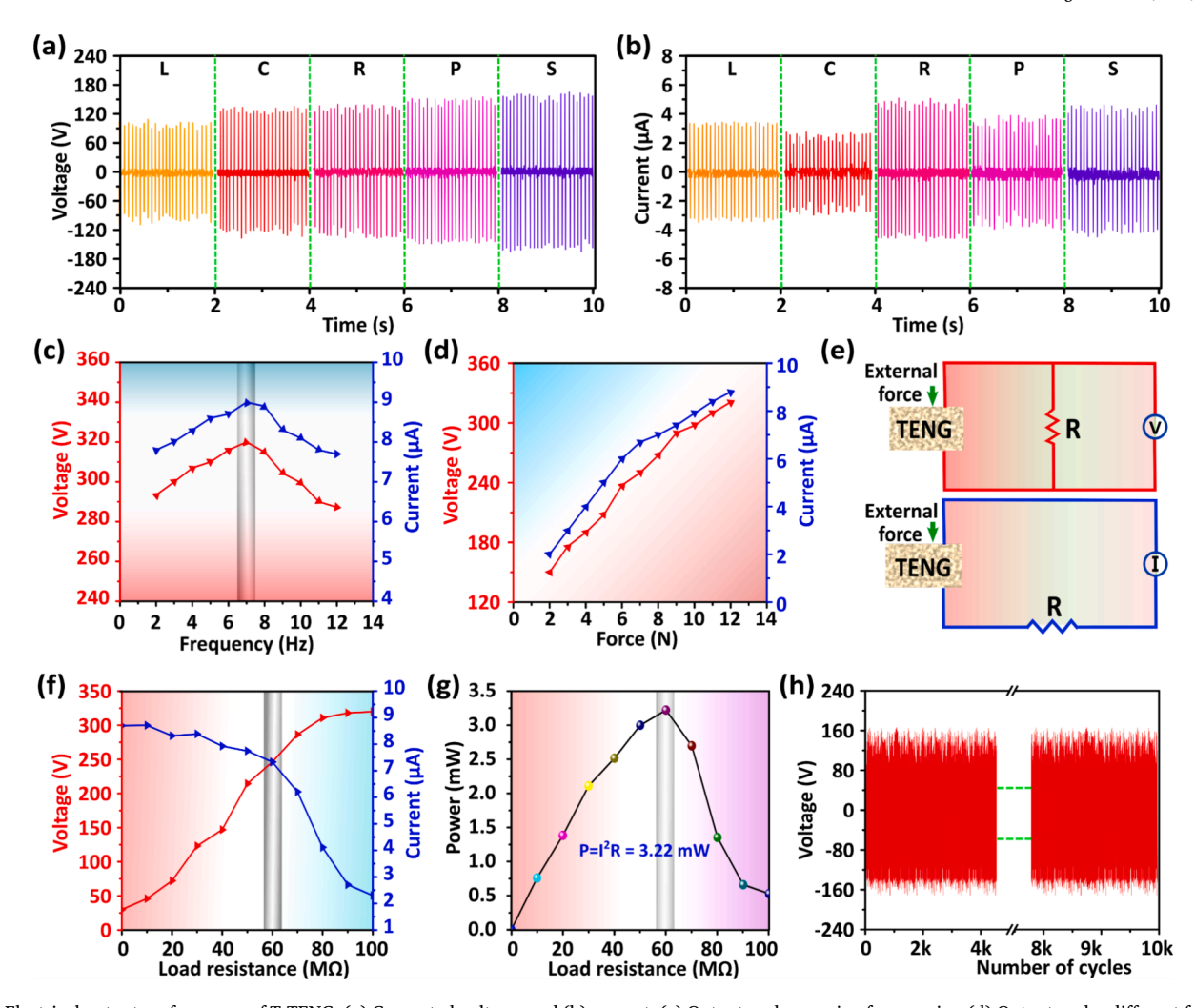


Fig. 4. Electrical output performance of T-TENG: (a) Generated voltage, and (b) current. (c) Output under varying frequencies. (d) Output under different forces. (e) Circuit for voltage and current measurement. (f) Output with varying load resistance. (g) Generated power. (h) Stability test.

3. Results and discussion

3.1. Surface morphological and elemental analysis

The surface morphology of the recycled textile layers (L, C, R, P, and S) used for T-TENG fabrication, was analyzed using Scanning Electron Microscopy (SEM). The SEM images of the frictional layers are provided in both lower and higher resolution (top and bottom Fig. 2a), respectively. The L layer showed a non-stiff arrangement of yarns via SEM image, providing flexibility that enhances the contact area and charge transfer efficiency during mechanical deformation. However, the lack of consistency and density in contact points may limit significant charge transfer, affecting TENG output performance. The SEM image of the C layer shows a non-uniform fabric arrangement with larger gaps between the fabric bunches, reducing the effective contact area, charge generation and transfer efficiency of the device (Xia et al., 2022). The R layer also has a non-uniform arrangement but with smaller distances between fabric bunches, resulting in a higher density of contact points that can enhance charge transfer, with potential variability in performance. The SEM image of P layer exhibits a non-stiff yarn arrangement and relatively small gaps between bunches, promotes better contact and flexibility, improving triboelectric interactions and overall TENG efficiency (Dhanabalan et al., 2019).

The SEM image of the S layer shows a smooth and uniform fabric arrangement, ensuring consistent and stable contact areas, leading to reliable and high triboelectric performance due to efficient and

consistent charge transfer (Ye et al., 2020). Therefore, the morphological characteristics observed via SEM directly influence the triboelectric performance of the fabricated devices.

Energy-Dispersive X-ray Spectroscopy (EDS) was employed to analyze the elemental composition of textile layers (L, C, R, P, and S). The EDS results consistently identified carbon (C) and oxygen (O) elements across the samples. Since S is a protein fiber, the EDS spectrum reveals the presence of Nitrogen beside the C and O (Karan et al., 2018; Yang et al., 2019) as shown in Fig. 2b, respectively. C is renowned for its favorable triboelectric properties, facilitating efficient charge transfer during mechanical contact and separation (Jayababu and Kim, 2021). As the C content increases, there is a corresponding potential enhancement in the material's ability to generate and transfer charges. Thus, the EDS analysis highlights the critical role of C content in determining the triboelectric performance of TENGs.

3.2. Working mechanism

The fundamental working principle of TENGs involves a combination of contact electrification and electrostatic induction. Contact electrification generates static polarized charges, while electrostatic induction transforms mechanical energy into electricity (Wang and Wang, 2019; Zhang et al., 2014). The schematic illustration of the T-TENG device is shown in Fig. 3a indicating the tribo-pairs of the device consist of recycled cloth samples and PVC layer, with Al foil tape as the electrodes. The distance (d) between these layers can change under

applied mechanical force. When the layers come into contact, their surfaces gain opposite static charges due to contact electrification (Fig. 3b). Additionally, Al electrodes installed within the TENG system ensure that charges can only transfer between the electrodes through external circuits. Once the external force is removed, the frictional layer starts to separate in a distance d(t), causing the charges to flow between electrodes (Fig. 3c). If we define the transferred charges from one electrode to another as O, one electrode will have a charge of -O and the other + Q, creating a potential difference between them. This electrical potential difference is influenced by the polarized triboelectric charges, contributing a voltage V(d,t) that depends on the separation distance d (t), and the transferred charges Q, contributing -Q/C(d,t), where C is the capacitance between the electrodes. To balance this potential difference, the electric field produced by the triboelectric charges prompts electrons flow through the external circuit, leading to the accumulation of charges on the electrode, represented. Additionally, this can lead to the generation of pulsed currents in external circuits (Lei et al., 2020). Further, the total voltage difference between the electrodes can be expressed as $V_{Total} = V(d,t) - Q/C(d,t)$

The device reaches saturation, indicated by zero charge transfer, when the friction layers attain their maximum separation distance of 2 cm, as depicted in Fig. 3d. Furthermore, upon re-application of the external force, the negative charges on the top electrode transfer to the bottom electrode, generating a reverse pulse current, as illustrated in Fig. 2e. This flow of charges will drop to zero through the external circuit once both layers are completely attached to each other. Thus, continuous contact-separation causes the alternating current (AC) generation by the T-TENG devices.

3.3. Electrical output performance of T-TENG

The electrical performance of T-TENGs fabricated from various recycled textile materials was systematically evaluated by measuring the output voltage and current. To better comprehend the impact of textile properties on the output performance of T-TENGs, properties such as mass per unit area, thickness, and yarn density were analyzed. The mass per unit area of the textiles used in T-TENGs was calculated using the formula m = W/A where W is the weight and A is the area of the sample. It was found to be 18.75, 15.62, 19.37, 21.87, and 23.75 g/m^2 for L, C, R, P, and S layers, respectively. The detailed calculations are provided in Note S1 Supporting Information. The textile materials used for device fabrication have thicknesses of 0.05, 0.02, 0.04, 0.05, and 0.06 cm, and yarn densities of about 82, 62, 78, 89, and 102 threads/cm² for L, C, R, P, and S, respectively. These properties directly influence the triboelectric charge density, mechanical properties, surface area for charge generation, consistency, and uniformity, all of which are vital for optimizing the device's performance and durability (Somkuwar and Kumar, 2023). Fig. 4a displays the voltage signals generated by the devices, showing an ascending order for the TENGs composed of L, C, R, P, and S layers, respectively. The highest output voltage was achieved by the device with the S layer, attributed to its higher surface charge density, resulting in higher voltage generation when in contact with other materials in TENG applications (Cao et al., 2024; Liu et al., 2022). In contrast, the highest output current was achieved by the device with the R layer, attributed to its higher charge transfer efficiency, which results in greater current generation (Cui et al., 2020; Liu et al., 2021) (Fig. 4b). Understanding these electrical output behavior further aids in selecting suitable materials for specific TENG applications. The fundamental principle underpinning this phenomenon involves the transfer of charges between two Al electrodes, facilitated by the potential difference arising from their contact and separation. Employing a controlled experimental setup, where a consistent contact area of 4 cm x 4 cm was maintained, periodic contact and separation were induced via manual tapping using a custom-made linear motor (Figure S2, Supporting Information). The experimental configuration involved connecting the positive probe terminal to the upper Al electrode and the negative

Table 1
Electrical output performance of the T-TENGs with different recycled textile samples.

Frictional layers		Electrode	Output performance			
Тор	Bottom		Voltage (V)	Current (µA)		
PVC	L	Al	226.54	6.63		
	С		250.35	5.29		
	R		266.87	9.11		
	P		300.92	7.98		
	S		320.76	8.73		

terminal to the lower electrode, thereby establishing a forward connection. This setup facilitated the precise measurement of peak-to-peak voltage and current, with the results subsequently cataloged in Table 1. Notably, the S-TENG generated a peak-to-peak output voltage of 320.76 V and a current of 8.73 μA , which was utilized for further electrical characterizations and applications. The output performance of the device was investigated under varying operational frequencies ranging from 2 to 12 Hz. The results showed that both the output voltage and current increased with increasing operational frequency, reaching their peak values at 7 Hz (Fig. 4c). This peak performance is attributed to the resonance frequency of the S-TENG device (Amini et al., 2023), where the mechanical vibrations are most efficiently converted into electrical energy.

However, beyond this optimal frequency, the output performance begins to decrease due to the rapid contact and separation, which prevents the layers from achieving their maximum separation distance, thereby reducing the overall output performance of the TENG device. Further, the output performance of the device was assessed under varying externally applied forces to evaluate its efficiency in converting mechanical motion into electricity. Using a force sensor, the applied force was varied from 2 to 12 N. The results showed that both the generated voltage and current increased with the increase in applied force (Fig. 4d). This indicates that the device is highly effective at converting mechanical energy into electrical energy. Further experimental investigations extended to analyze the S-TENG's output performance under varying load conditions. This was accomplished by connecting electrical loads of different resistance values, ranging from 10 to 100 $M\Omega$, to the device and meticulously measuring the resultant output voltage and current. The circuit connections for measuring voltage and current are provided in schematic Fig. 4e, with the top part illustrating the voltage measurement setup and the bottom part depicting the current measurement configuration. The results showed that the generated voltage of the device increased with increasing load resistance, while the current decreased, consistent with Ohm's law (Sagade Muktar Ahmed et al., n.d.).

The voltage and current curves intersect at 60 M Ω , indicating the optimal load resistance of the device as shown in Fig. 4f. This represents the balance where the device can achieve its maximum power output, demonstrating its efficiency under varying electrical load conditions. In addition, the generated power of the device was calculated using the formula, $P = I^2R$ where I is the instantaneous current and R is the respective load resistance. The maximum power generated by the device was found to be 3.22 mW which is sufficient to power small-scale electronics (Fig. 4g). Further, the generated power density of the device is calculated using the formula $P_{Dens} = P/A$ where P is the generated power and A is the effective contact area of the fabricated device. The power density of the optimized device is found to be 2.01 W/m². The electrical stability of the device was assessed through 10,000 cycles of operation. The corresponding voltage signals in Fig. 4 h indicate that the voltage remains constant throughout the cycles, demonstrating the device's mechanical durability and electrical stability. Furthermore, to assess long-term durability and electrical stability of S-TENG, the output voltage and current of the device was evaluated over 5 months, finding consistent performance throughout the testing period, ensuring their

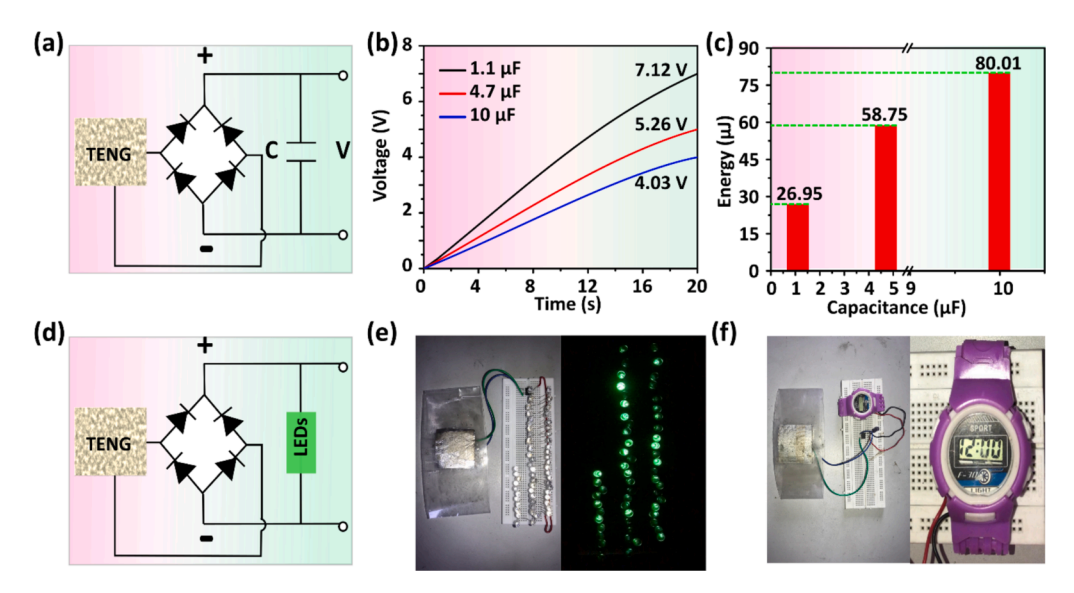


Fig. 5. (a) Circuit diagram for charging capacitor. (b) Capacitor charging curves. (c) Energy stored in each capacitor. (d) Circuit diagram for powering LEDs. (e) Device connection and glowing LEDs. (f) Photographic portrayal of the circuit connection and powering smartwatch using T-TENG.

practical viability and sustainability in real-world applications (Figure S1 Supporting Information). This comprehensive analysis not only elucidates the electrical performance characteristics of T-TENGs across different textile layers but also provides insights into their behavior under diverse conditions, thereby contributing to the broader understanding of T-TENG operational dynamics.

3.4. Life cycle assessment

Conducting a life cycle assessment (LCA) for recycled textile fabrics used in TENGs involves evaluating the environmental impacts across different stages of the product's life. It begins with the raw material extraction phase, where discarded or post-consumer textiles composed of L, C, R, P, and S were collected from tailor shops as the primary source. These textiles then undergo a recycling process, which involves sorting by material type, cleaning to remove contaminants, and preparing the fabric for further processing. Once recycled, the fabric is processed and transformed into functional layers for TENGs using metal components for electrodes.

During the recycling and manufacturing stages, energy consumption is a key factor, and both the energy used in recycling the textiles and the energy required to convert them into TENG layers are included in the assessment. Emissions generated during transportation and production processes are accounted for in the energy and emission inputs. Additionally, the water footprint of textile recycling, including water used in washing and any chemical treatments, is thoroughly evaluated. Waste outputs, such as residual waste from rejected fabrics or scrap materials during the manufacturing process, are also considered in the LCA.

The transportation phase evaluates the environmental impact of moving recycled textiles to processing sites and distributing the final TENG product. Trade-offs between increased energy demand during recycling and the reduced material extraction from virgin resources are analyzed. Recycled textiles offer enhanced recyclability, allowing the possibility of further recycling or energy recovery, which contributes to the reduction of waste. The disposal of electronic components in TENGs, such as electrodes, is carefully considered, with an emphasis on minimizing electronic waste.

The lifetime of textiles varies widely based on the type, usage, environmental conditions, and maintenance. For example, under normal conditions, the estimated lifespan is approximately 10 years for L, 3 years for C and R, 5 years for P, and 2 years for S (Gonzalez et al., 2023; Islam et al., 2021). For textile-based TENGs, the lifespan is influenced by

factors such as mechanical stress, moisture, temperature fluctuations, and chemical exposure, which can shorten their durability (Li et al., 2023; Liman et al., 2022).

By using recycled materials, we significantly reduce textile waste, aligning with circular economy principles (Christensen, 2021; Saha et al., 2022). As TENGs are self-powered systems, they provide sustainable energy generation with minimal ongoing resource use. Compared to virgin textile-based TENGs, recycled textile TENGs can reduce the environmental burden of fabric production, leading to a more sustainable approach to energy harvesting. The detailed LCA underscores the environmental advantages of using recycled textiles in TENGs and provides a clearer understanding of their overall environmental impact.

4. Applications

The application of a TENGs for energy harvesting represents a significant advancement in the realm of renewable energy, utilizing the triboelectric effect to transform mechanical energy into electrical energy (Trinh and Chung, 2023). However, TENGs naturally produce alternating current (AC), which cannot be used directly to power electronic devices that require direct current (DC). Therefore, a rectifier bridge is employed to convert the AC output of the S-TENGs into DC, as illustrated in Fig. 5a. This rectified output from the S-TENG is then used to charge three distinct electrolytic capacitors with capacitances of 1.1 µF, 4.7 µF, and 10 µF. These capacitors are observed to be charged to voltages of 7.12 V, 5.26 V, and 4.23 V respectively, as shown in Fig. 5b. The energy stored in each capacitor can be calculated using the formula E =1/2 CV², where C is the capacitance, and V is the voltage. Based on this formula, the stored energies are determined to be 26.95 μJ for the 1.1 μF capacitor, 58.75 μJ for the 4.70 μF capacitor, and 80.01 μJ for the 10 μF capacitor within 20 s, as illustrated in Fig. 5c. Further, the device is demonstrated to power a series of green LEDs. The circuit used for this purpose is depicted in Fig. 5d. The practical implementation, with the S-TENG connected to the rectifier bridge and the series of 57 LEDs, and the visual evidence that the device is capable of powering the entire series of 57 LEDs are provided in Fig. 5e and Supporting Video S1. Further, to demonstrate its practical application, the device is utilized to power a smartwatch without the use of any external battery (Fig. 5f, and Supporting Video S2). This illustrates the potential of T-TENGs to serve as a sustainable and efficient energy source for low-power electronic devices. The capability to convert mechanical energy from movements or

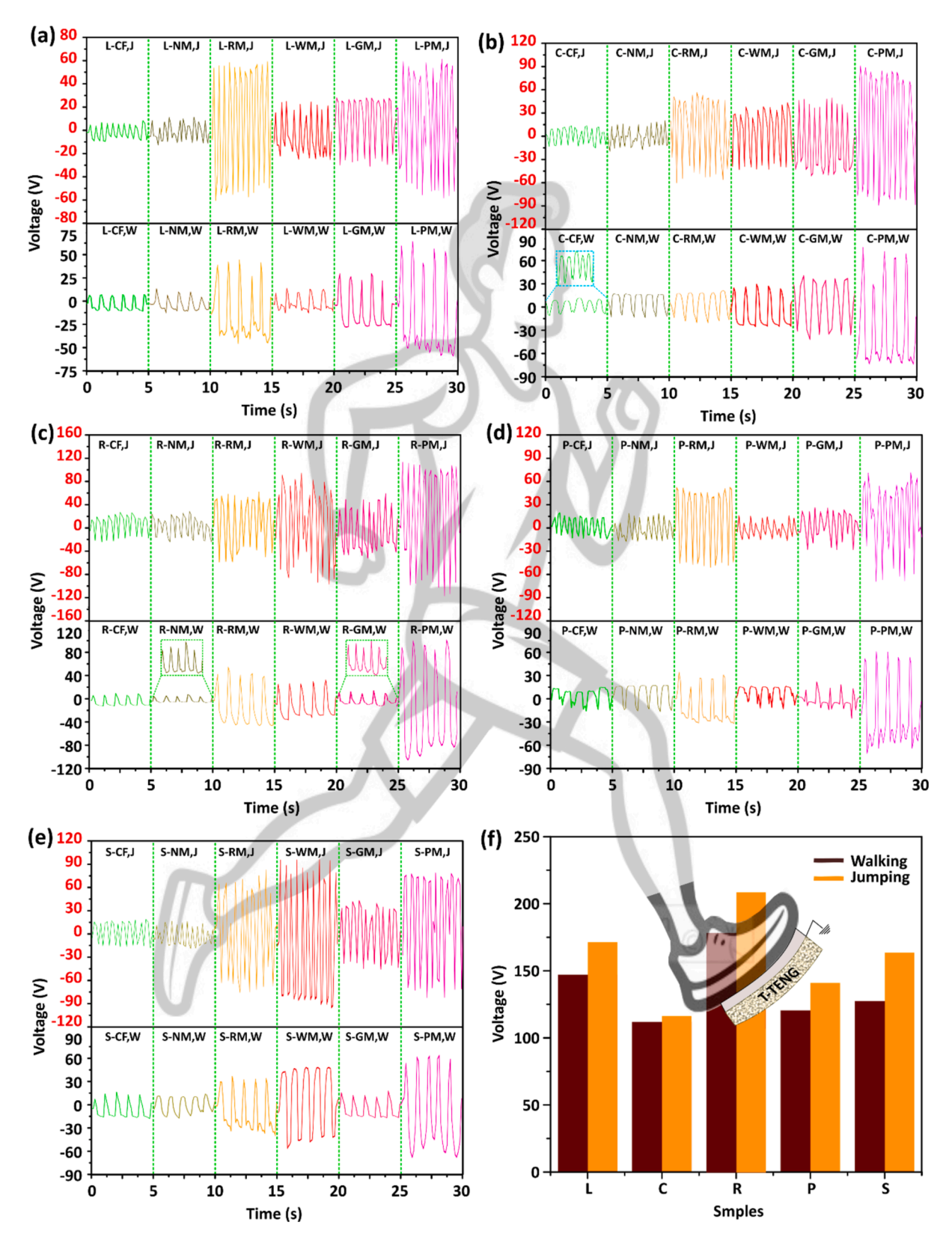


Fig. 6. (a-e) The generated voltage signals of T-TENGs for each fabric sample. (f) Comparative analysis.

vibrations into usable electrical energy, store it effectively, and then utilize it to power electronic components demonstrates the versatility and efficacy of T-TENG technology in practical applications.

To demonstrate the real-time application of the fabricated T-TENGs, composed of various fabrics namely L, C, R, P, and S, were configured in

a single-electrode mode to harness biomechanical energy. These T-TENG devices were ingeniously integrated into the insoles of shoes, allowing them to generate voltage from the mechanical energy produced by walking (W) and jumping (J) (Supporting video S3 and S4, respectively). The performance of these devices was tested on six different

Table 2The electrical output performance of T-TENG in single electrode mode.

Samples	Energy harvesting form	Output voltage generated using different contact materials						
		Concrete floor	Nylon mat	Rubber mat	Woolen mat	Gel-foam mat	PVC coil mat	
L	Walking	12.03	19.96	87.32	23.01	51.64	111.79	
	Jumping	18.21	38.43	119.10	46.36	53.88	116.24	
С	Walking	20.25	22.25	32.66	57.16	68.33	147.21	
	Jumping	25.57	30.03	104.05	80.81	86.44	171.34	
R	Walking	23.45	15.85	85.38	48.55	18.25	178.41	
	Jumping	26.84	44.84	104.63	126.70	54.19	208.52	
P	Walking	26.82	30.90	59.03	21.95	30.99	120.47	
	Jumping	29.23	34.92	99.30	33.91	40.42	140.95	
S	Walking	32.19	23.89	66.14	99.44	29.97	127.39	
	Jumping	36.43	28.94	158.89	177.31	76.75	163.51	

surfaces including concrete floor (CF), nylon mat (NM), rubber mat (RM), woolen mat (WM), gel-foam mat (GM), and PVC coil mat (PM). The generated voltage signals from T-TENG devices using L, C, R, P, and S as the triboactive layer are shown in Fig. 6a to 6e, respectively. These figures indicate that the devices consistently produced higher output voltages under jumping conditions compared to walking, with the PM being the most effective surface. The detailed output performance of these devices is presented in Table 2, which reveals the superior performance of the R-fabric-based device.

Specifically, this device generated an impressive 178.41 V during walking and 208.52 V during jumping on the PM, as illustrated in Fig. 6f. The circuit connection is provided in the inset of Fig. 6f, with a more detailed version in Figure S3 Supporting Information. This novel application showcases the versatility and practical utility of T-TENG technology. By embedding T-TENGs into the insoles of shoes, it becomes feasible to harvest energy from routine activities such as walking and jumping. This integration transforms ordinary movements into a sustainable energy source, highlighting the potential of T-TENGs in wearable technology.

Further, the ability of these devices to generate substantial voltage, particularly when using R on a PM, underscores their potential for high-efficiency energy harvesting. The use of various fabrics demonstrates the adaptability of T-TENGs to different materials, optimizing the triboelectric effect based on the application. The high output voltage achieved by the R-fabric-based T-TENG suggests that the material properties of R, combined with the triboelectric characteristics of the PM, create an optimal environment for energy generation. Furthermore, the practical implementation of T-TENGs in shoe insoles points to a wide range of potential applications in wearable technology, from powering small electronic devices to serving as a supplementary energy source for portable gadgets. The real-world setup, detailed in the figures and tables, provides a clear validation of the technology's effectiveness and efficiency.

5. Conclusions

The present work successfully demonstrated the fabrication and characterization of Textile-based Triboelectric Nanogenerators (T-TENGs) using various recycled textiles. Five T-TENGs were fabricated using various recycled fabrics (L, C, R, P, and S) as tribopositive materials and PVC as tribonegative material and Al foil tape as electrode. SEM analysis was conducted to explore the surface morphology of the textile layers while EDS analysis has been performed to determine the elemental composition of textile layers. SEM revealed distinct yarn arrangements in these textile layers, which directly influence triboelectric performance. EDS analysis identified carbon (C) and oxygen (O) in all samples, with carbon content increasing from L to S. The electrical output performance of the T-TENG devices was systematically evaluated. Among the samples, the S-TENG achieved the highest output voltage of 320.76 V and a current of 8.73 μA . Additionally, the device was utilized to charge various electrolytic capacitors and power a series

of 57 LEDs. T-TENG applications were explored by integrating the devices into shoe insoles to harvest biomechanical energy from walking and jumping on different surfaces. The rayon-based T-TENG showed the highest voltage generation, reaching up to 208.52 V during jumping on a PVC coil mat, demonstrating its potential for wearable technology and energy harvesting applications. Therefore, the present study not only addresses energy needs by extracting energy from recycled textiles but also offers a sustainable solution to mitigate the environmental impact associated with textile waste accumulation.

6. Declaration of generative AI

During the preparation of this work, the authors used ChatGPT to improve language and readability. After using this tool, the authors reviewed and edited the content as needed and take full responsibility for the content of the publication.

CRediT authorship contribution statement

Sebghatullah Amini: Writing – original draft, Visualization, Software, Methodology, Investigation, Formal analysis, Data curation, Conceptualization. Rumana Farheen Sagade Muktar Ahmed: Writing – review & editing, Visualization, Validation, Formal analysis. Santosh Kumar: Writing – review & editing. Sangamesha Madanahalli Ankanathappa: Validation, Resources, Methodology. Krishnaveni Sannathammegowda: Supervision.

Declaration of competing interest

The authors declare that they have no known competing financial interests or personal relationships that could have appeared to influence the work reported in this paper.

Acknowledgments

Sebghatullah Amini is financially supported by the Indian Council for Cultural Relations (ICCR) scholarship, the Government of India. Rumana Farheen S.M. acknowledges the Council of Scientific and Industrial Research (CSIR), Government of India, for the financial assistance provided under the Research Associate fellowship (File no. 364-4194-9498/2K23/1).

Appendix A. Supplementary data

Supplementary data to this article can be found online at https://doi. org/10.1016/j.wasman.2024.10.013.

Data availability

Data will be made available on request.

References

- Agrawal, R., Sharan, M., 2015. Municipal textile waste and its management. Res. J. Fam. community Consum. Sci. 3, 4–9.
- Ahmed, R.F.S.M., Mohan, S.B., Ankanathappa, S.M., Shivanna, M., Basith, S.A., Shastry, M.H.C., Chandrasekhar, A., Sannathammegowda, K., 2023. Sucrose assisted chemical-free synthesis of rGO for triboelectric nanogenerator: Green energy source for smart-water dispenser. Nano Energy 106, 108085.
- Ahmed, R.F.S.M., Amini, S., Ankanathappa, S.M., Sannathammegowda, K., 2024. Electricity out of electronic trash: Triboelectric nanogenerators from discarded smartphone displays for biomechanical energy harvesting. Waste Manag. 178, 1–11.
- Alves, D.I., Barreiros, M., Fangueiro, R., Ferreira, D.P., 2024. Valorization of textile waste: non-woven structures and composites. Front. Environ. Sci. 12, 1365162.
- Amini, S., Ahmed, R.F.S.M., Ankanathappa, S.M., Shastry, M.H.C., Shivanna, M., Sannathammegowda, K., 2024. Investigating the Annealing Effects on the Performance of Polyvinyl alcohol-Graphite-based Triboelectric Nanogenerator. Sensors Actuators A Phys. 115309.
- Amini, S., Sagade Muktar Ahmed, R.F., Madanahalli Ankanathappa, S., S, K., 2023. Polyvinyl alcohol-based Economical Triboelectric Nanogenerator for Self-powered Energy Harvesting Applications. Nanotechnology.
- Arafat, H.A., Jijakli, K., 2013. Modeling and comparative assessment of municipal solid waste gasification for energy production. Waste Manag. 33, 1704–1713.
- Athanasopoulos, P., Zabaniotou, A., 2022. Post-consumer textile thermochemical recycling to fuels and biocarbon: A critical review. Sci. Total Environ. 834, 155387.
- Candido, R.G., 2021. Recycling of textiles and its economic aspects, in: Fundamentals of Natural Fibres and Textiles. Elsevier, pp. 599–624.
- Cao, C., Li, Z., Shen, F., Zhang, Q., Gong, Y., Guo, H., Peng, Y., Wang, Z.L., 2024. Progress on techniques for improving output performance of triboelectric nanogenerators. Energy Environ, Sci.
- Chen, X., Jiang, T., Yao, Y., Xu, L., Zhao, Z., Wang, Z.L., 2016. Stimulating acrylic elastomers by a triboelectric nanogenerator–toward self-powered electronic skin and artificial muscle. Adv. Funct. Mater. 26, 4906–4913.
- Christensen, T.B., 2021. Towards a circular economy in cities: Exploring local modes of governance in the transition towards a circular economy in construction and textile recycling. J. Clean. Prod. 305, 127058.
- Cui, X., Zhang, Y., Hu, G., Zhang, L., Zhang, Y., 2020. Dynamical charge transfer model for high surface charge density triboelectric nanogenerators. Nano Energy 70, 104513.
- Dhanabalan, S.C., Dhanabalan, B., Chen, X., Ponraj, J.S., Zhang, H., 2019. Hybrid carbon nanostructured fibers: Stepping stone for intelligent textile-based electronics. Nanoscale 11, 3046–3101.
- Dickson, M.A., Loker, S., Eckman, M., 2014. Social responsibility in the global apparel industry. Bloomsbury Publishing USA.
- Dong, K., Wu, Z., Deng, J., Wang, A.C., Zou, H., Chen, C., Hu, D., Gu, B., Sun, B., Wang, Z. L., 2018. A stretchable yarn embedded triboelectric nanogenerator as electronic skin for biomechanical energy harvesting and multifunctional pressure sensing. Adv. Mater. 30, 1804944.
- Dong, K., Peng, X., Cheng, R., Ning, C., Jiang, Y., Zhang, Y., Wang, Z.L., 2022a. Advances in high-performance autonomous energy and self-powered sensing textiles with novel 3D fabric structures. Adv. Mater. 34, 2109355.
- Dong, K., Peng, X., Cheng, R., Wang, Z.L., 2022b. Smart textile triboelectric nanogenerators: prospective strategies for improving electricity output performance. Nanoenergy Adv. 2, 133–164.
- Gonzalez, V., Lou, X., Chi, T., 2023. Evaluating environmental impact of natural and synthetic fibers: a life cycle assessment approach. Sustainability 15, 7670.
- Huygens, D., Foschi, J., Caro, D., Caldeira, C., Faraca, G., Foster, G., Solis, M., Marschinski, R., Napolano, L., Fruergaard Astrup, T., 2023. Techno-scientific assessment of the management options for used and waste textiles in the. European Union. Joint Research Centre (Seville site).
- Islam, J.M.M., Mondal, M.I.H., Das, S.C., 2021. The life and durability issues of natural textiles and clothing, in: Fundamentals of Natural Fibres and Textiles. Elsevier, pp. 657–690.
- Jayababu, N., Kim, D., 2021. Co/Zn bimetal organic framework elliptical nanosheets on flexible conductive fabric for energy harvesting and environmental monitoring via triboelectricity. Nano Energy 89, 106355. https://doi.org/10.1016/j. nanoen.2021.106355.
- Jiang, J., Kang, X., Zheng, G., Ye, H., Cui, T., Fan, W., Xiong, H., Zhang, M., Ge, S., 2023.
 An innovative remedy to transform plastic waste and used paper box into high-performance biocomposite. J. Mater. Res. Technol. 26, 4121–4132.
- Juanga-Labayen, J.P., Labayen, I.V., Yuan, Q., 2022. A review on textile recycling practices and challenges. Textiles 2, 174–188.
- Karan, S.K., Maiti, S., Kwon, O., Paria, S., Maitra, A., Si, S.K., Kim, Y., Kim, J.K., Khatua, B.B., 2018. Nature driven spider silk as high energy conversion efficient biopiezoelectric nanogenerator. Nano Energy 49, 655–666.
- Khandaker, S., Bashar, M.M., Islam, A., Hossain, M.T., Teo, S.H., Awual, M.R., 2022. Sustainable energy generation from textile biowaste and its challenges: a comprehensive review. Renew. Sustain. Energy Rev. 157, 112051.

- Köksal, D., Strähle, J., Müller, M., Freise, M., 2017. Social sustainable supply chain management in the textile and apparel industry—A literature review. Sustainability 9, 100.
- Kumar, P., Samuchiwal, S., Malik, A., 2020. Anaerobic digestion of textile industries wastes for biogas production. Biomass Convers. Biorefinery 10, 715–724.
- Lei, R., Shi, Y., Ding, Y., Nie, J., Li, S., Wang, F., Zhai, H., Chen, X., Wang, Z.L., 2020. Sustainable high-voltage source based on triboelectric nanogenerator with a charge accumulation strategy. Energy Environ. Sci. 13, 2178–2190.
- Li, J., Cai, J., Yu, J., Li, Z., Ding, B., 2023. The rising of fiber constructed piezo/ triboelectric nanogenerators: from material selections, fabrication techniques to emerging applications. Adv. Funct. Mater. 33, 2303249.
- Li, X., Wang, L., Ding, X., 2021. Textile supply chain waste management in China. J. Clean. Prod. 289, 125147.
- Liman, M.L.R., Islam, M.T., Hossain, M.M., 2022. Mapping the progress in flexible electrodes for wearable electronic textiles: materials, durability, and applications. Adv. Electron. Mater. 8, 2100578.
- Liu, W., Wang, Z., Hu, C., 2021. Advanced designs for output improvement of triboelectric nanogenerator system. Mater. Today 45, 93–119.
- Liu, L., Zhao, Z., Li, Y., Li, X., Liu, D., Li, S., Gao, Y., Zhou, L., Wang, J., Wang, Z.L., 2022. Achieving Ultrahigh Effective Surface Charge Density of Direct-Current Triboelectric Nanogenerator in High Humidity. Small 18, 2201402.
- Niinimäki, K., Peters, G., Dahlbo, H., Perry, P., Rissanen, T., Gwilt, A., 2020. The environmental price of fast fashion. Nat. Rev. Earth Environ. 1, 189–200.
- Nunes, L.J.R., Godina, R., Matias, J.C.O., Catalão, J.P.S., 2018. Economic and environmental benefits of using textile waste for the production of thermal energy. J. Clean. Prod. 171, 1353–1360.
- Paosangthong, W., Torah, R., Beeby, S., 2019. Recent progress on textile-based triboelectric nanogenerators. Nano Energy 55, 401–423.
- Roy Choudhury, A.K., 2013. Green chemistry and the textile industry. Text. Prog. 45, 3–143.
- Sagade Muktar Ahmed, R.F., Gangadharan, A.K., Amini, S., Mohan, S.B., Ankanathappa, S.M., Shankaregowda, S.A., Sannathammegowda, K., n.d. Economical Polypropylene-Based Triboelectric Nanogenerator for Self-powered Biomechanical Sensor Application. Phys. status solidi.
- Saha, K., Dey, P.K., Papagiannaki, E., 2022. Implementing circular economy in the textile and clothing industry, in: Supply Chain Sustainability in Small and Medium Sized Enterprises. Routledge, pp. 239–276.
- Senthil Kumar, P., Suganya, S., 2017. Toxic free supply chain for textiles and clothing. Detox Fash. Supply Chain 1–25.
- Somkuwar, V.U., Kumar, B., 2023. Influence of the fabric topology on the performance of a textile-based triboelectric nanogenerator for self-powered monitoring. ACS Appl. Polym. Mater. 5, 2323–2335.
- Stanescu, M.D., 2021. State of the art of post-consumer textile waste upcycling to reach the zero waste milestone. Environ. Sci. Pollut. Res. 28, 14253–14270.
- Trinh, V.-L., Chung, C.-K., 2023. Advances in Triboelectric Nanogenerators for Sustainable and Renewable Energy: Working Mechanism, Tribo-Surface Structure, Energy Storage-Collection System, and Applications. Processes 11, 2796.
- Wagaw, T., Babu, K.M., 2023. Textile Waste Recycling: A Need for a Stringent Paradigm Shift. AATCC J. Res. 10, 376–385.
- Wang, Y., 2010. Fiber and textile waste utilization. Waste and biomass valorization 1, 135-143.
- Wang, Z.L., Wang, A.C., 2019. On the origin of contact-electrification. Mater. Today 30, 34–51.
- Wang, W., Yu, A., Zhai, J., Wang, Z.L., 2021. Recent progress of functional fiber and textile triboelectric nanogenerators: towards electricity power generation and intelligent sensing. Adv. Fiber Mater. 3, 394–412.
- Xia, R., Zhang, R., Jie, Y., Zhao, W., Cao, X., Wang, Z., 2022. Natural cotton-based triboelectric nanogenerator as a self-powered system for efficient use of water and wind energy. Nano Energy 92, 106685.
- Yang, H., Yu, Z., Li, K., Jiang, L., Liu, X., Deng, B., Chen, F., Xu, W., 2019. Facile and effective fabrication of highly UV-resistant silk fabrics with excellent laundering durability and thermal and chemical stabilities. ACS Appl. Mater. Interfaces 11, 27426–27434.
- Ye, H., Jiang, J., Yang, Y., Shi, J., Sun, H., Zhang, L., Ge, S., Zhang, Y., Zhou, Y., Liew, R. K., 2023. Ultra-strong and environmentally friendly waste polyvinyl chloride/paper biocomposites. Adv. Compos. Hybrid Mater. 6, 81.
- Ye, C., Xu, Q., Ren, J., Ling, S., 2020. Violin string inspired core-sheath silk/steel yarns for wearable triboelectric nanogenerator applications. Adv. Fiber Mater. 2, 24–33.
- Yousef, S., Eimontas, J., Striūgas, N., Tatariants, M., Abdelnaby, M.A., Tuckute, S., Kliucininkas, L., 2019. A sustainable bioenergy conversion strategy for textile waste with self-catalysts using mini-pyrolysis plant. Energy Convers. Manag. 196, 688–704
- Zhang, C., Tang, W., Han, C., Fan, F., Wang, Z.L., 2014. Theoretical comparison, equivalent transformation, and conjunction operations of electromagnetic induction generator and triboelectric nanogenerator for harvesting mechanical energy. Adv. Mater. 26, 3580–3591.